Biotechnology Reports 26 (2020) e00469

Contents lists available at ScienceDirect

Biotechnology Reports

journal homepage: www.elsevier.com/locate/btre

Plant extract mediated synthesis enhanced the functional properties of silver ferrite nanoparticles over chemical mediated synthesis

Harshiny Muthukumar, Santosh Kumar Palanirajan, Manoj Kumar Shanmugam, Sathyanarayana N. Gummadi*

Applied and Industrial Microbiology Lab, Department of Biotechnology, Indian Institute of Technology Madras, Chennai, 600036, India

ARTICLE INFO

Article history:
Received 7 February 2020
Received in revised form 15 April 2020
Accepted 11 May 2020

Keywords:
Silver ferrite
Nanoparticles
Cytotoxicity
Antibacterial activity

ABSTRACT

In this study, the antibacterial, antioxidant and cytotoxicity behaviour of silver ferrite nanoparticles (AgFeO2 NPs) synthesized through chemical and green routes were compared.

Green synthesis (Bio) of AgFeO2 NPs were prepared by precipitation method using Amaranthus blitum leaves extract as a reducing agent. Chemical synthesis (Che) of AgFeO2 NPs was mediated by sodium borohydride as a reducing agent. [AgFeO2 (Bio)] NPs showed reduced size, better monodispersity and surface area compared to [AgFeO2 (Che)] NPs. The results showed that synthesized NPs have better antibacterial activity against E. coli than S. aureus. In addition, 250 μg of AgFeO2 (Bio) and (Che) NPs showed antioxidant efficiency of 98 and 86%. The results showed that [AgFeO2 (Bio)] NPs showed lower cytotoxicity [AgFeO2 (Che)] NPs against human human embryonic kidney (HEK 293) cells. These results suggest that [AgFeO2 (Bio)] NPs have improved physicochemical properties thereby they can be used as an effective biocatalytic material in biotechnology.

1. Introduction

In current eons, the development of multifunctional material is of great significance to solve serious environmental and public healthcare problem by pathogenic microorganisms and toxic compounds [1]. Various treatment methods and materials have been studied to overcome the major cause of chronic infections and mortality due to microbes [2,3]. In this regard, the nanomaterials such as nanoparticles (NPs), nanofibers, metal–oxide nanocomposites, nano-hybrid crystals have virtuous properties such as higher chemical and thermal stability [4–6]. These characteristic of NPs makes it very useful in various field such as biomedical sciences, cosmetics, clinical, environmental and renewable energy technologies [7]. Among the various types of nanomaterials, silver (Ag) NPs have better antimicrobial activity and has been extensively used as a disinfectant in many products including food, textiles and crop protection [8–10]. However, Ag NPs has drawbacks such as adverse noxious effect, problem of aggregation, and less magnetic property. Thus, recovering and recycling of Ag nanoparticles is especially difficult in practical applications [9,11].

To overcome these problems and improve the magnetic property, Ag NPs can be blended with ferrite, magnetic (FeO_2) NPs to improve the separation efficacy. These combinations enhance the Ag NPs functions such as aggregation, recycling and reusability of materials [12,13]. Likewise, functionalization of FeO_2 NPs with metals such as Au, Ag, Cu, Ag, Pd, Pt has confirmed immense application in catalysis and biotechnology [14]. Among the composite $AgFeO_2$ are highly attractive due to its catalytic, magnetic and electrical traits. Recently, $AgFeO_2$ NPs was considered to be a promising photocatalyst owing to NPs narrow band gap and magnetic properties as well as $AgFeO_2$ NPs can be reused after degradation process [15]. $AgFeO_2$ magnetic composites have been successfully synthesized by researchers and used as an efficient antibacterial agent [16]. Formerly, $AgFeO_2$ composite NPs were synthesized through several methods such as sol–gel, co-precipitation, hydrothermal, pulsed laser deposition and thermolysis method [17,18]. But, all of these methods engaged high temperature and pressure conditions and long reaction times [19]. Also, NPs prepared by above methods have toxicity, less stability, monodispersity, high solubility, and leaching problem; thus limits NPs usage in real time applications [20]. In the view of these drawback finding of novel material is crucial.

Several researchers have been reported that biotic synthesis of NPs using microbes such as bacteria, algae, fungi, yeast, virus and plants [7,21,22]. Among several biological mediated syntheses of NPs, microbe mediated synthesis is not of practically achievable due to

* Corresponding author.
E-mail address: gummadi@iitm.ac.in (S.N. Gummadi).

https://doi.org/10.1016/j.btre.2020.e00469

the requirements of extremely sterile atmosphere and maintenance. Thus, the plant extract mediated synthesis were more convenient over microorganisms owe to ease processing, a lesser amount of biohazard involvement and maintaining cell cultures [23,24]. It has been reported that biological materials such as plant source extract and amino acid mediated synthesis changed the chemical nature of the noxious NPs as well as easy to synthesize [25]. Many researchers studied that plant extracts mediated NPs synthesis was nontoxic, low cost, stable, also extensively used in many fields [7]. It has been reported that compared to chemical mediated synthesis, plant extract mediated FeO and Ag NPs holds better particles size, band gap and enhanced stability, monodispersity [7,20,26]. Previously, it has been stated that plant like Amaranth family plant leaves extract mediated NPs showed enhanced antimicrobial activities, ability to form biofilms, exhibited improved photocatalytic activity and less toxicity. In addition, leaf extracts did not create any toxic by-products compared to chemical mediated synthesis [10,24]. It was confirmed that Amaranth family plant extract was an alternate cost-effective and nontoxic reducing agent for synthesizing NPs [20,26]. Amid amaranth family, *Amaranthus blitum* L., holds a high amount of ascorbic acid, carotene, riboflavin, niacin and thiamine. The plants are generally applied as a dressing to treat swellings, irritations and lung disorders [27]. With this perception, this study reports silver ferrite ($AgFeO_2$) NPs were synthesized by green co-reduction method using *A. blitum* leaf extract as a reducing agent and compounds such as iron (III) nitrate ($Fe(NO_3)_3{\cdot}9H_2O$), silver nitrate ($AgNO_3$) were used as a precursor.

In this study, $AgFeO_2$ NPs were prepared by both chemical co-reduction precipitation method using $NaBH_4$ as well as by green co-reduction using *A. blitum* leaf extract. $AgFeO_2$ NPs by two methods were compared for the first time in terms of structure, size, shape, surface area and magnetic properties using various analytical techniques. Hereafter, green *A. blitum* leaves extract and chemical $NaBH_4$ mediated AgFeO NPs was referred to as [AgFeO (Bio)] and [$AgFeO_2$ (Che)] NPs respectively. In addition, the antioxidant activity of leaf extract, [$AgFeO_2$ (Bio)] and [$AgFeO_2$ (Che)] NPs were analyzed using 1, 1- diphenyl-2-picrylhydrazyl (DPPH) radical scavenging test. The disk diffusion method and minimum inhibitory concentration (MIC) were conducted to evaluate the qualitative and quantitative antibacterial tendency of [AgFeO (Bio)] and [$AgFeO_2$ (Che)] NPs against *Staphylcoccus aureus* (Gram- positive) and *Escherichia coli* (Gram- negative).

2. Materials and method

2.1. Materials

The test organisms *Escherichia coli* (MTCC 7410) and *Staphylococcus aureus* (MTTC 424)were obtained from the Microbial Type Culture Collection, Chandigarh, India. Compounds such as iron (III) nitrate ($Fe(NO_3)_3{\cdot}9H_2O$), silver nitrate ($AgNO_3$), sodium borohydride ($NaBH_4$) hydrochloric acid (HCl), sodium hydroxide (NaOH) dimethyl sulfoxide (DMSO) methanol, α, α-diphenyl-β-picrylhydrazyl (DPPH), ascorbic acid, kanamycin, nutrient agar were procured from Merck and Himedia, India. Dulbecco's modified eagle's medium (DMEM), penicillin-streptomycin-neomycin solution, fetal bovine serum (FBS) were purchased from Thermofischer Scientific (New York, USA), 3-(4,5-dimethylthiazol-2-yl)-2,5-diphenyltetrazolium bromide (MTT) assay kit and dimethyl sulfoxide (DMSO) were procured from Himedia Laboratories (Mumbai, India).

2.2. Preparation of leaf extract

Initially, *A. blitum* leaves were collected, then washed with double distilled water to eliminate unwanted adhering substance and chopped into small-size pieces. Then 25 g of *A. blitum* leaves were extracted with 100 ml of milli Q water at 55 ± 2 °C in soxhlet extractor till the exhaustion. Lastly, the leaf extract was filtered by vacuumfiltration with a buchner funnel (Whatman No.1 filter paper). The procedure reported by Sarker and Oba 2020 was followed to estimates *A. blitum* leaf extract total antioxidant capacity (TAC) using DPPH and total phenolic content (TPC) by Folin–Ciocalteu reagent (FCR). Ascorbic acid and gallic acid were used as standard for TAC and TPC estimation [28]. The obtained leaf extract was used for AgFeO NPs synthesis and the filtrate was stored in a refrigerator (4 °C) for further use.

2.3. Synthesis of A. blitum leaves extract and $NaBH_4$ mediated $AgFeO_2$ NPs

[$AgFeO_2$ (Bio)] NPs was prepared by co-precipitation method [18]. Briefly, 0.1 mmol $Fe(NO_3)_3{\cdot}9H_2O$ and 0.1 mmol $AgNO_3$ were dissolved in 75 ml of milli Q water. The solution mixture was stirred at room temperature for 15 min. Then, 25 ml of prepared leaf extract (pH 9.0) was added to the mixture drop by drop with constant stirring at 300 rpm using magnetic stirrer at 50 ± 2 °C for 3 h. The colour changes from dark yellow to colourless solution with dark brown precipitate was confirmed the formation of [$AgFeO_2$ (Bio)] NPs. Then, the obtained precipitates were collected by sedimentation, washed using absolute ethanol and three times in milli Q water to remove unreacted impurities and dried at 50 ± 2 °C for 6 h. Likewise, for comparison [$AgFeO_2$ (Che)] NPs was synthesized with the same procedures but instead of plant extract; 25 ml of 0.1 M $NaBH_4$ solution (pH 9.0) as a reducing agent. The possible mechanism of $AgFeO_2$ NPs formation by $NaBH_4$ and *A. blitum* extract mediated synthesis was shown in scheme S1. After drying, $AgFeO_2$ NPs in the form of flakes was then powdered using agate mortar and pestle, obtained [$AgFeO_2$ (Bio)] and [$AgFeO_2$ (Che)] NPs were stored in bottles for further application and characterization [20].

2.4. Characterization

The synthesized $AgFeO_2$ NPs absorption spectra were obtained using UV–vis spectrophotometer (Shimadzu UV-1800 Kyoto, Japan) over a wavelength range of 200–800 nm. IR spectra of aqueous leaf extracts and $AgFeO_2$ NPs were recorded by fourier transform infrared spectroscopy (FTIR- Thermo Scientific99 ^{TM} Inc. Nicolet^{TM} iS^{TM}5, USA) over a spectral range of 400–4000 cm^{-1} with a resolution of 4 cm^{-1} at room temperature. Crystalline structure and phase identification of AgFeO NPs were confirmed from X-ray diff ;raction (XRD) pattern recorded using Rigaku Ultima III powder X-ray diff ;raction, Japan. The XRD pattern was recorded at θ–2θ geometry with $CuK_{\alpha 1}$ (1.5406 Å) at 40 kV and 30 mA over the range of 10° to 70° with a step size of 0.02°. AgFeO NPs zeta potential and size distribution of the NPs were investigated using Horiba SZ-100 nanopartica, Japan). Before examination, NPs were dispersed in deionized water (pH 7 ± 0.1) and sonicated for 3 min. Three replicates were performed for obtaining standard values of prepared samples. Magnetic measurements of AgFeO NPs carried out using vibrating sample magnetometer (VSM) Lakeshore 7404 (Westerville OH). Scanning electron microscope (SEM) with energy dispersive spectrometer (EDS) JOEL 6700 F, Japan at 30 kV was used to see the morphology and elemental composition of NPs

2.5. Determination of the minimum inhibitory concentration (MIC), agar disk diffusion and DPPH Assay

The minimum concentration of $AgFeO_2$ NPs that shows antibacterial activity was quantified. The MIC was determined by batch cultures containing varying concentrations (0–100 μg/mL) of

$AgFeO_2$ NPs in suspension. The antibacterial activity of synthesized $AgFeO_2$ NPs against *Staphylococcus aureus* (Gram-positive), and *Escherichia coli* (Gram-negative) using Kirby–Bauer Disk Diffusion vulnerability assessment method [19,24]. DPPH assay was followed to estimate the free radical scavenging activity of A.blitum leaves extract, [$AgFeO_2$ (Bio)] and [$AgFeO_2$ (Che)] NPs were determined by using nitrogen- centred DPPH scavenging assay [29]. The statistical significance of these experiment was determined using GraphPad Prism software (La Jolla, CA, USA) column analysis, one-way ANOVA.

2.6. Cytotoxicity evaluation

Tetrazolium salt (3-(4,5-Dimethylthiazol-2-yl)-2,5-diphenyltetrazolium bromide (MTT) based cytotoxicity assay were carried out with the synthesized nanoparticles. Briefly non-cancerous human embryonic kidney cells (HEK 293T) were allowed to grow in 25 cm^2 cell culture flask till 90 % confluent at 37 °C in a 5 % CO_2 incubator. The cells were then seeded into each well of 96 well microculture plate and grown for 24 h and treated with the NPs synthesized by appropriate methods namely [$AgFeO_2$ (Bio)] and [$AgFeO_2$ (Che)] NPs and FeO_2 (Bio) and FeO_2 (Che) NPs uniformly suspended in 10 % DMSO in different concentrations ranging from 20 μg to 100 μg. Cells incubated with 10 % DMSO was used as control. After incubation period of 24 h MTT solution was added to each well at a final concentration of 1 mg/ml and incubated for 4 h in the dark. Then the insoluble formazan was dissolved with the solubilization buffer provided with the kit. The assay was performed in triplicate and OD was measured at 570 nm.

3. Results and discussion

3.1. UV–vis spectral studies

The absorbance spectrum of synthesized [$AgFeO_2$ (Bio)] and [$AgFeO_2$ (Che)] NPs. was analyzed the wavelength ranges from 200 to 900 nm by UV–Vis spectrophotometry was shown in (Fig. 1A). The absorbance peak at 214 nm confirmed the existence of phenolic compounds in the leaf extract (data not shown). UV–vis absorption of the synthesized NPs dissolved in DMSO shows small plasmon shift as well as broadening at 356 nm and small absorption peak nearly at 242 nm which is due to the presence of $AgFeO_2$ nanocomposite. In addition, when comparing the synthesized [$AgFeO_2$ (Bio)] and [$AgFeO_2$ (Che)] NPs with bare Ag and FeO_2 NPs nanoparticles the absorption spectrum showed a peak at 391 nm and 214 nm respectively [30]. The optical properties of pure FeO and Ag NPs were studied by UV/Vis spectroscopy (data not shown). It illustrates pure FeO NPs spectrum does not show definite absorption maxima wavelength range from 300 to 800 nm. Similarly, Ag NPs does not show any maximum absorption at 200 to 300 nm. Likewise Berastegui et al., reported UV–Vis measurements of $AgFeO_2$NPs show a strong absorptions from 300 to 650 nm [31]. Thus, broadening of absorption at 356 nm in (Fig. 1A) were owing to the presence of $AgFeO_2$ NPs.

3.2. FTIR studies

The functional groups of the active components in leaf extracts and potential chemical variations owe to the creation of $AgFeO_2$ NPs were studied using FT-IR spectroscopic analysis. The bonding configurations of *A. biltum* were studied using FTIR with the spectral range from 400 to 4000 cm^{-1} as shown in the (Fig. 1B). The intense broad band detected from 3352–3232 cm^{-1} assigned to the H-bonded and O—H stretching vibration of phenolic and hydroxyl group of leaf extract. The sharp peaks appeared on 1636 cm^{-1} indicates the presence of primary amine NH— bend. The slight shift was detected around 2080 cm^{-1} denote —CC =—stretch variable. The peaks at 1360 cm^{-1} and 1324 cm^{-1} were assigned to alkane C—H stretch and aromatic amine CN— stretch. FTIR analysis also confirm the presence of functional groups (CO— stretch) such as carboxylic acid, ester, ether; which shows the peak values at 1084–1012 cm^{-1}. The peaks from 820 and 664 cm^{-1} are due to CH— (aromatic) bond. In addition, from TAC and TPC estimation the prepared leaf extract 25/100 ml shows 75 μg gallic acid equivalent (GAE) activity and 80 μg ascorbic acid equivalent DPPH radical scavenging capacity. These, TAC, TPC estimation and IR functional groups indicate the existence of polyphenols, alkaloids and flavonoids of leaf extracts. The bioactive compounds in *A. blitum* extract are used to reduce the metal ions into respective metal [27]. Sarker and Oba 2020 reported that *A. blitum* leafy vegetables is abundant sources of antioxidant phytopigments, vitamin C, β-carotene, phenolics, minerals and proximate [28]. Moreover, these phytochemicals have highly reactive hydroxyl groups; that provide hydrogen to reduce the free radicals. The antioxidant and reducing activity were similar molecular mechanisms [20]. The result confirms that these phytochemicals were believed to play a role in bio-reduction reaction.

Further, experiments are required for the clarification of real mechanism and the biochemical pathway to assess the formation of NPs by plant extract. But, the feasible formation mechanism of

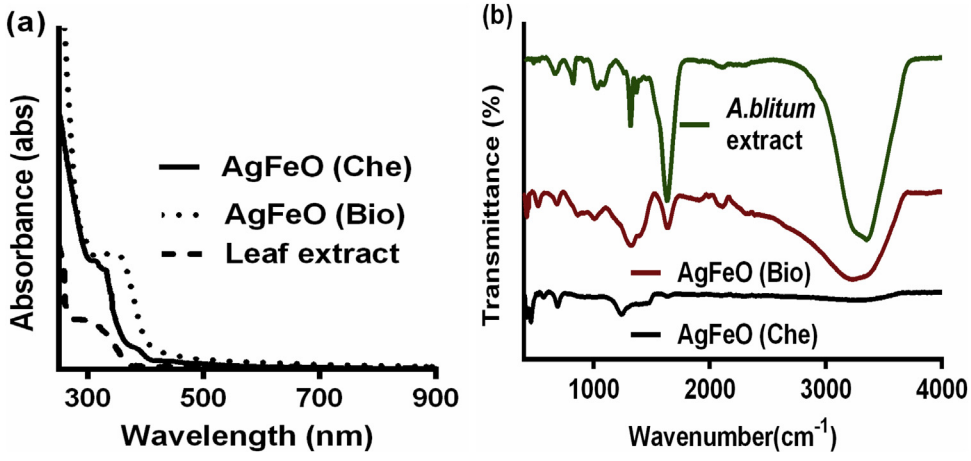

Fig. 1. Spectral analysis of *A. blitum* aqueous leaf extract, biological and chemical mediated $AgFeO_2$ NPs. (a) Comparison of leaf extract, biological and chemical mediated $AgFeO_2$ NPs UV–vis analysis. The samples were scanned from 200 nm to 900 nm in 1.00 cm path length cuvettes. (b) FTIR spectral analysis of leaf extract, [$AgFeO_2$ (Bio)] and [$AgFeO_2$ (Che)] NPs. obtained over the range of 400 - 4000 cm^{-1} with a resolution of 4 cm^{-1} at room temperature.

$AgFeO_2$ NPs using *A. blitum* leaf extract and $NaBH_4$ were conferred in scheme S1 (see supplementary). The IR spectrum and phytochemical analysis confirmed that plant extract having polyphenol group. It was believed that phenol group in *A. blitum* extract reduce the metal ions into respective metal and stabilization of metal. The IR spectrum of [$AgFeO_2$ (Bio)] NPs show the suppression of aliphatic compounds in NPs, can be ascribed to the changes such as redox reaction of the phytochemical compounds during the [$AgFeO_2$ (Bio)] NPs formation (Fig. 1B). Also, IR results showing that organic groups from leaf were attached to the [$AgFeO_2$ (Bio)] NPs surface, which evidently confirmed that *A. biltum* leaf extract was acted as a stabilizer for the formation of NPs. The peak that appeared in the $AgFeO_2$ (Bio) at 520, 412 cm^{-1} is due to the iron oxide skeleton (–O–Fe), representing the existence of $AgFeO_2$ NPs [32]. It was also reported that the adsorption of reducing agents on the surface of metallic nanoparticles is due to the presence of organic compound functional groups present in their molecular structures.

Similarly, scheme S1 clearly indicated that mechanism behind the synthesis of [$AgFeO_2$ (Che)] NPs. At 50 °C, Fe $(NO_3)_3$ and $AgNO_3$ metal precursor reduced by $NaBH_4$, resulting in the formation of $AgFeO_2$ and sub products. Then reaction product has undergone separation and purification to obtained [$AgFeO_2$ (Che)] NPs. The appearance of two peaks around 544 and 466 cm^{-1} in (Fig. 1b) may be due to the stretching vibrations of the Ag-O bonds and the Fe-O bonds respectively in [$AgFeO_2$ (Che)] NPs. Similarly, it has been reported that $AgFeO_2$ prepared by facile precipitation method confirms the pure $AgFeO_2$ band at 586 cm^{-1} in IR spectra was due to the lattice vibrations of $AgFeO_2$ [33].

3.3. XRD structural analysis of NPs

The crystal structures of [$AgFeO_2$ (Bio)] and [$AgFeO_2$ (Che)] NPs were confirmed by XRD pattern, which is shown in (Fig. 2A). XRD patterns of the synthesized NPs revealed main sharp planes in the diffractogram, indicating that [$AgFeO_2$ (Bio)] and [$AgFeO_2$ (Che)] NPs were crystalline in nature. The peaks observed at 14.27, 28.77, 34.8, 37.07, 40.63, 43.78, 50.52, 56.89, 59.64, 60.9, 62.97, 63.25, 68.77 and 72.09 were matching to the diffraction peaks of 2H polytype hexagonal $AgFeO_2$. The distinct planes, possibly indexed to (002), (004), (101), (102), (103), (006), (105), (106), (008), (110), (112), (107) (114) and (201) were observed for NPs sample [9]. Durham, et al., reported that $AgFeO_2$ synthesized via precipitation route mostly form a mixture of 3R and 2H delafossite $AgFeO_2$ structure [34]. In addition trace impurities likes hydroxides, Ag and Ag_2O were also found to be in $AgFeO_2$ NPs synthesized by precipitation method [31]. Markedly, $AgFeO_2$ diffraction patterns do not show presence of additional impurities also there is no significant existence 3R phase (Fig. 2A). Thus, the $AgFeO_2$ peaks corresponded to JCPDS card no. 25-0765. The peaks indexing might be assigned to the 2H phase resulted in a lattice parameter unit cell with a(Å) = 3.0390, b (Å) = 3.390, c (Å) = 12.395 besides small intensity difference was found between the NPs can be owed to the leaf extract bio-compounds bound to [AgFeO (Bio)] NPs surface [20,26]

3.4. VSM analysis

The magnetic properties of [$AgFeO_2$ (Bio)] and [$AgFeO_2$ (Che)] NPs are analyzed using VSM. The magnetization of the $AgFeO_2$ samples measurements were verified by VSM at room temperature are shown in (Fig. 2B) illustrates a hysteresis loop of [$AgFeO_2$ (Bio)] and [$AgFeO_2$ (Che)] NPs. It revealed that saturation magnetization values were found to 87.7 emu/g for $AgFeO_2$ (Che) and 80.7 emu/g for $AgFeO_2$ (Bio). The magnetic property of [$AgFeO_2$ (Bio)] was lesser than [$AgFeO_2$ (Che)] NPs. The materials magnetic properties were mainly depending on various features such as crystallinity, size and surface coating. Hence, presence of plant extract residues in [$AgFeO_2$ (Bio)] can reduce NPs saturation magnetization values [18]. Casbeer et al., reported that ferrite NPs were highly stable and it have unique magnetic properties. Hence, recovery of NPs from the medium is very facile; due to this magnetic properties synthesized NPs are believed to effectively useful in many applications such as adsorbents, catalysts and antimicrobial agents [35].

3.5. SEM studies and EDX measurements

Morphology of [$AgFeO_2$ (Bio)] and [$AgFeO_2$ (Che)] NPs prepared through facile and single-step reaction were investigated using SEM as shown in (Fig. 3A and B). The [$AgFeO_2$ (Bio)] NPs seemingly illustrated mono-dispersed and less aggregation micrograph. In contrast, (Fig. 3B) of [$AgFeO_2$ (Che)] NPs appeared in more aggregated form. It was noted that both [$AgFeO_2$ (Bio)] and [$AgFeO_2$ (Che)] NPs were looked like spherical morphology. Moreover, SEM micrograph depicted that [$AgFeO_2$ (Bio)] NPs have better

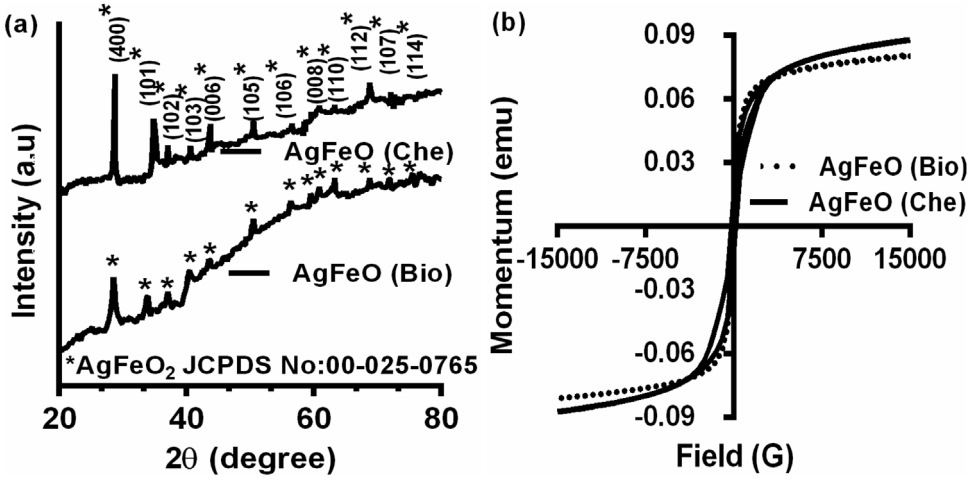

Fig. 2. X-ray diffraction and Vibrating sample magnetometer analysis (a) XRD pattern of biological and chemical mediated $AgFeO_2$ NPs [$AgFeO_2$ (Bio)] and [$AgFeO_2$ (Che)] NPs XRD pattern were recorded using Cu K α radiation in the angular range of 2θ from 20 to 80 °. Diffractogram of NPs also corresponded to JCPDS card no:00-025-0765 $AgFeO_2$. (b) Vibrating sample magnetometer (VSM) analysis of Synthesized [AgFeO2 (Bio)] and [$AgFeO_2$ (Che)] NPs magnetization curves obtained by VSM measurement at room temperature with a magnetic field of −15,000 to 15,000 G.

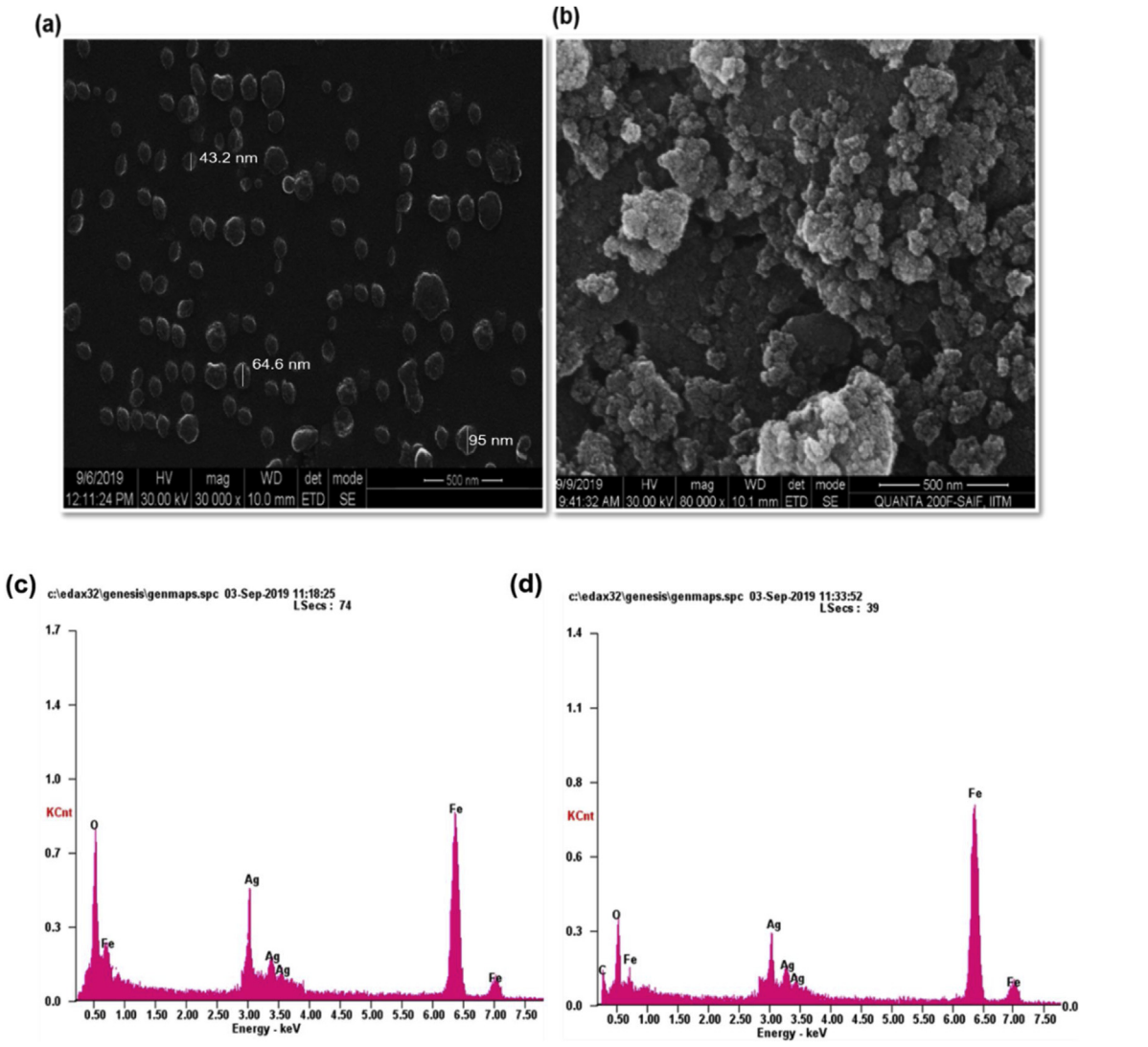

Fig. 3. Scanning electron micrograph of synthesized NPs (a,b) SEM images of [$AgFeO_2$ (Bio)] and [$AgFeO_2$ (Che)] NPs at 500 nm resolution respectively, The samples were prepared by a drop-dry method on glass slide and SEM operating at a voltage of 30 keV (c,d) corresponding energy dispersive X-ray spectra of NPs.

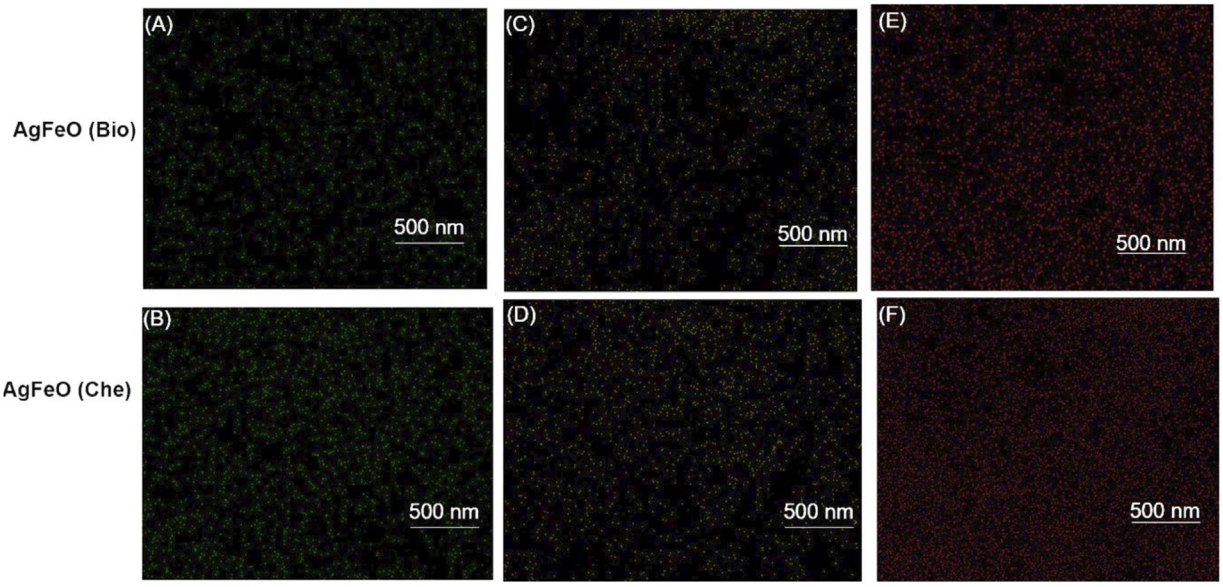

Fig. 4. EDX elemental analysis (a,b) Ag (c,d) Fe (e,f) O element mapping images of AgFeO (Bio) and (Che) NPs.

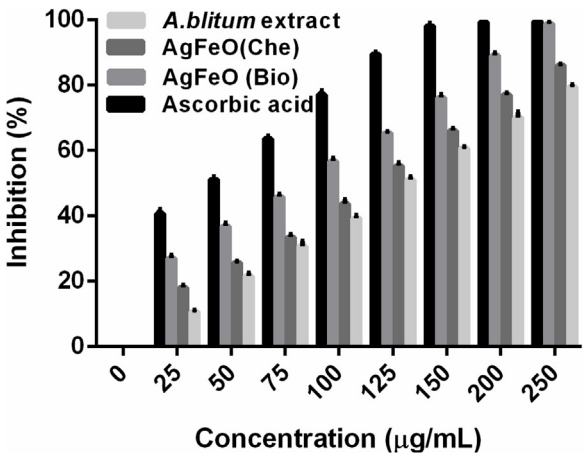

Fig. 5. Antioxidant activity by DPPH radical scavenging assay. DPPH scavenging activity of [AgFeO (Bio)] and [AgFeO (Che)] NPs compared with the standard ascorbic acid and prepared leaf extract. Results are representative of three replicates and error bars represent standard deviation. One-way ANOVAs were performed to evaluate significance comparing the both NPs to the control. A value of $p < 0.0001$ was considered to be statistically significant as compared to the control.

morphology and less agglomeration. It was due to leaf extract phyto-compounds acted as a stabilization agents [24]. The chemical composition of [$AgFeO_2$ (Bio)] and [$AgFeO_2$ (Che)] NPs were investigated by EDX analysis (Fig. 3C and D). The elemental analysis [$AgFeO_2$ (Bio)] and [$AgFeO_2$ (Che)] NPs illustrated that composition of Ag, Fe, and O. In addition, trace amount of C element was present in [$AgFeO_2$ (Bio)] NPs. The characteristic signals for Ag, O and Fe were apparently detected at 3, 0.3 KeV and 0.8 for Fe L_a, 6.5 Fe K_a and 7.0 Fe K_b, respectively. Furthermore, the composition of the Ag and Fe were tested in elemental EDX mapping. The mapping of Ag (green), Fe (yellow) and O (red) was shown in the (Fig. 4). The EDX elemental analysis in Fig. 4(a and b) Ag (c,d) Fe (e, f) O element mapping images of $AgFeO_2$ (Bio) and (Che) NPs clearly indicates that both Ag and Fe were homogeneously dispersed throughout [$AgFeO_2$ (Bio)] and [$AgFeO_2$ (Che)] NPs sample [36].

3.6. Charge and size analysis

The Table 1 depicted Zeta potential measurement of [$AgFeO_2$ (Bio)] and [$AgFeO_2$ (Che)] NPs were carried out at a neutral pH value. The [$AgFeO_2$ (Bio)] and [$AgFeO_2$ (Che)] NPs potential was observed to be -43.8 and -28.6 mV, respectively. Particle size analysis in Table 1 showed that average size of [$AgFeO_2$ (Bio)] NPs in 92 nm and [$AgFeO_2$ (Che)] NPs in 110 nm. This can be attributed to bio-molecules bound toward NPs surface that enhances its stability by preventing aggregation [24].

3.7. Antioxidant activity of NPs

The antioxidant activity of synthesized [$AgFeO_2$ (Bio)], [$AgFeO_2$ (Che)] NPs and aqueous *A. blitum* leaf extract was determined by using DPPH assay (Fig. 5). The free radical scavenging activity of NPs tends to increase with increasing its concentration, also both NPs have a significant inhibitory activity against the DPPH radicals. The NPs antioxidant activity was owed to the shifting of the electron in oxygen to the odd electron in oxygen surface orbits $^{\bullet}OH$ and $O_2^{\bullet-}$ radicals [26]. Notably, [$AgFeO_2$ (Bio)] NPs exhibits higher antioxidant activity of 99 % at 250 µg which is in comparison with control ascorbic acid (Fig. 5). The binding of bioactive constituents with [$AgFeO_2$ (Bio)] NPs enhanced the antioxidant activity also owed to small size of monodispersed NPs provide more number of active sites to scavenge the free radicals and inhibit the oxidation reactions [37]. Thus, the antioxidant activity of [$AgFeO_2$ (Bio)] NPs exhibited higher than [$AgFeO_2$ (Che)] NPs. In addition, leaf extract (250 µg) shows higher inhibition activity of 79.5 %. It was due to bioactive molecules in the leaf extract were decidedly reactive OH

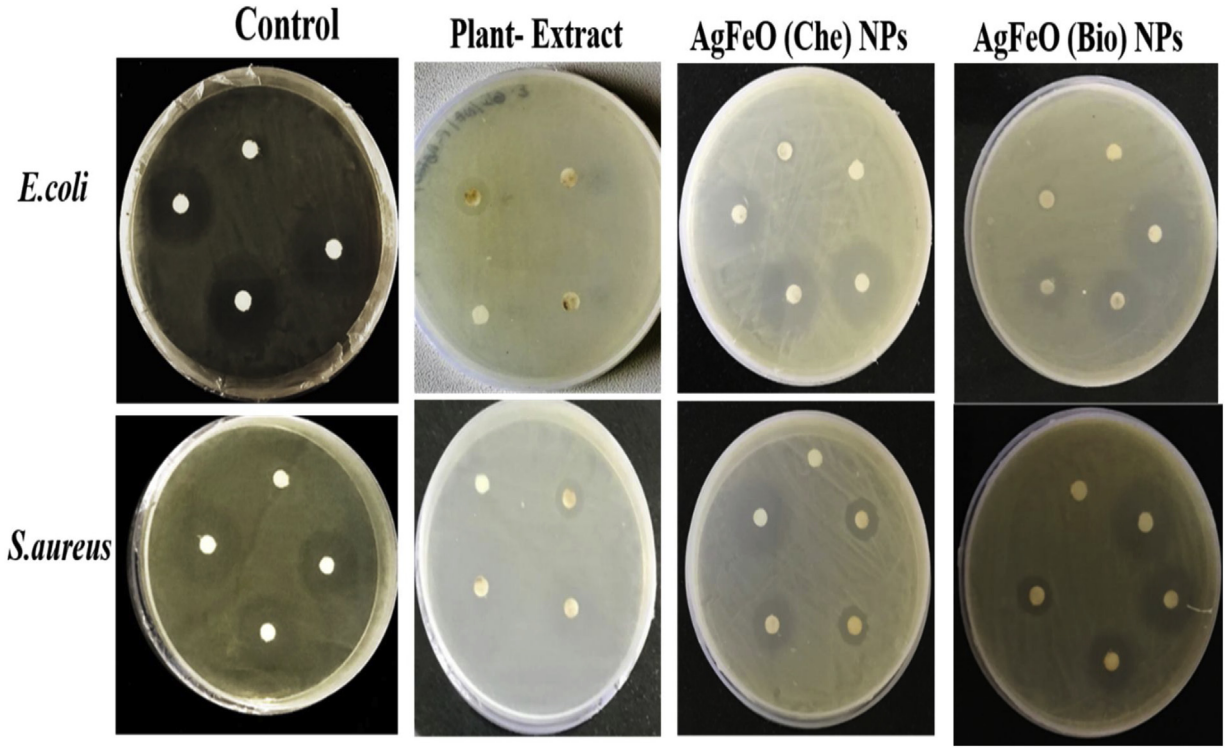

Fig. 6. Zone of inhibition (mm) against *E. coli* and *S. aureus* and various concentration (10,20 and 30 µg) of Kanamycin, prepared leaf extract, [AgFeO (Bio)] and [AgFeO (Che)] NPs. by disk diffusion method.

groups donate H to decrease the free radicals. The result confirms that reducing capacity of leaf extract was increased with increasing the antioxidant activity of leaf extract [20,26].

3.8. Disc diffusion

The various concentrations of 10, 20 and 30 μg of [$AgFeO_2$ (Bio)] and [$AgFeO_2$ (Che)] NPs were tested for antibacterial activity against *E. coli* and *S. aureus* by disc diffusion assay. (Fig. 6) illustrates ZOI diameter measurements for [$AgFeO_2$ (Bio)] and [$AgFeO_2$ (Che)] NPs, kanamycin and leaf extract. The results clearly represented that, the prepared [$AgFeO_2$ (Bio)] NPs exhibited higher antibacterial activity than [$AgFeO_2$ (Che)] NPs and leaf extract (Table S1). Also, beyond 30 μg of [$AgFeO_2$ (Bio)] showed zone of inhibition comparable to kanamycin (Fig. 7A and B). The better activity of [$AgFeO_2$ (Bio)] NPs was due to organic molecules on NPs surface and significantly rises NPs active site and stability by inhibiting accumulation than [$AgFeO_2$ (Che)] NPs [38].

3.9. Minimum inhibitory concentration (MIC)

Minimum quantity of NPs required for antibacterial activity was estimated by the standard MIC method. The results clearly showed that both [$AgFeO_2$ (Bio)] NPs and [$AgFeO_2$ (Che)] NPs have bactericidal efficiency on *E. coli* and *S. aureus* compared to leaf extract and kanamycin (Fig. 7C and D). Fig S2 (see supplementary) clearly showed that *E. coli* growth was inhibited by 98% and 83.9% in the presence of 100 μg [$AgFeO_2$ (Bio)] and [$AgFeO_2$ (Che)] NPs

Table 1
Shape, structure, zeta potential, particle size and saturation magnetization of AgFeO (Bio) and AgFeO (Che) NPs.

NPs	Shape	Structure	Zetapotential(mV)	Particle size(nm)	SaturationMagnetization(emu g-1)
A-AgFeO	Spherical	2H polytype hexagonal	−43.8	92.1	87.6
B-AgFeO	Spherical	2H polytype hexagonal	−28.6	110.5	80.86

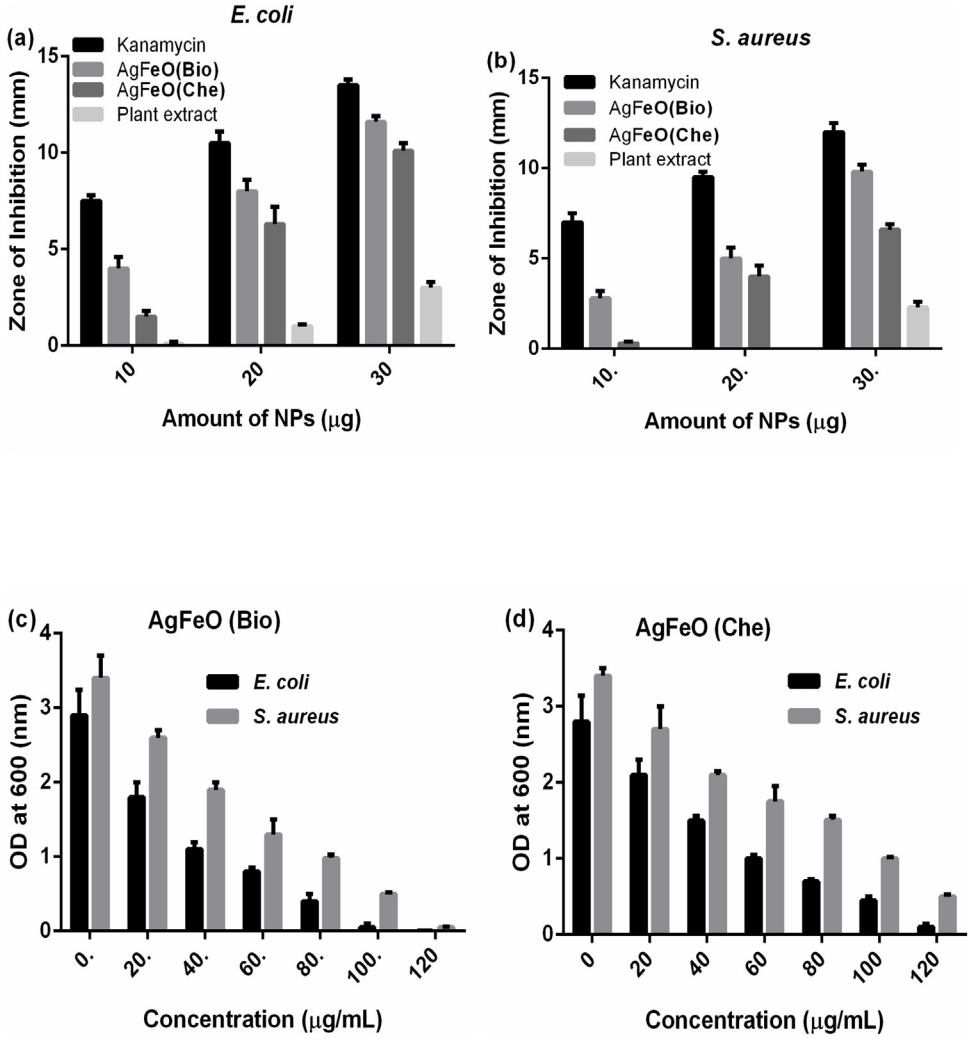

Fig. 7. Antibacterial activity of biological and chemical mediated $AgFeO_2$ NPs by agar disk-diffusion and broth dilution Assay (a, b) Zone of inhibition (mm) of various concentration (10,20 and 30 μg) of Kanamycin, prepared leaf extract, [$AgFeO_2$ (Bio)] and [$AgFeO_2$ (Che)] NPs against *E. coli* and *S. aureus* respectively. (c, d) Minimum inhibitor concentration (20, 40, 60, 80 and 100 μg) of [$AgFeO_2$ (Bio)] and [$AgFeO_2$ (Che)] NPs against *E. coli* and *S. aureus* respectively. One-way ANOVAs were performed to evaluate significance comparing the both NPs to the control. A value of $p < < 0.0001$was considered to be statistically significant as compared to the control.

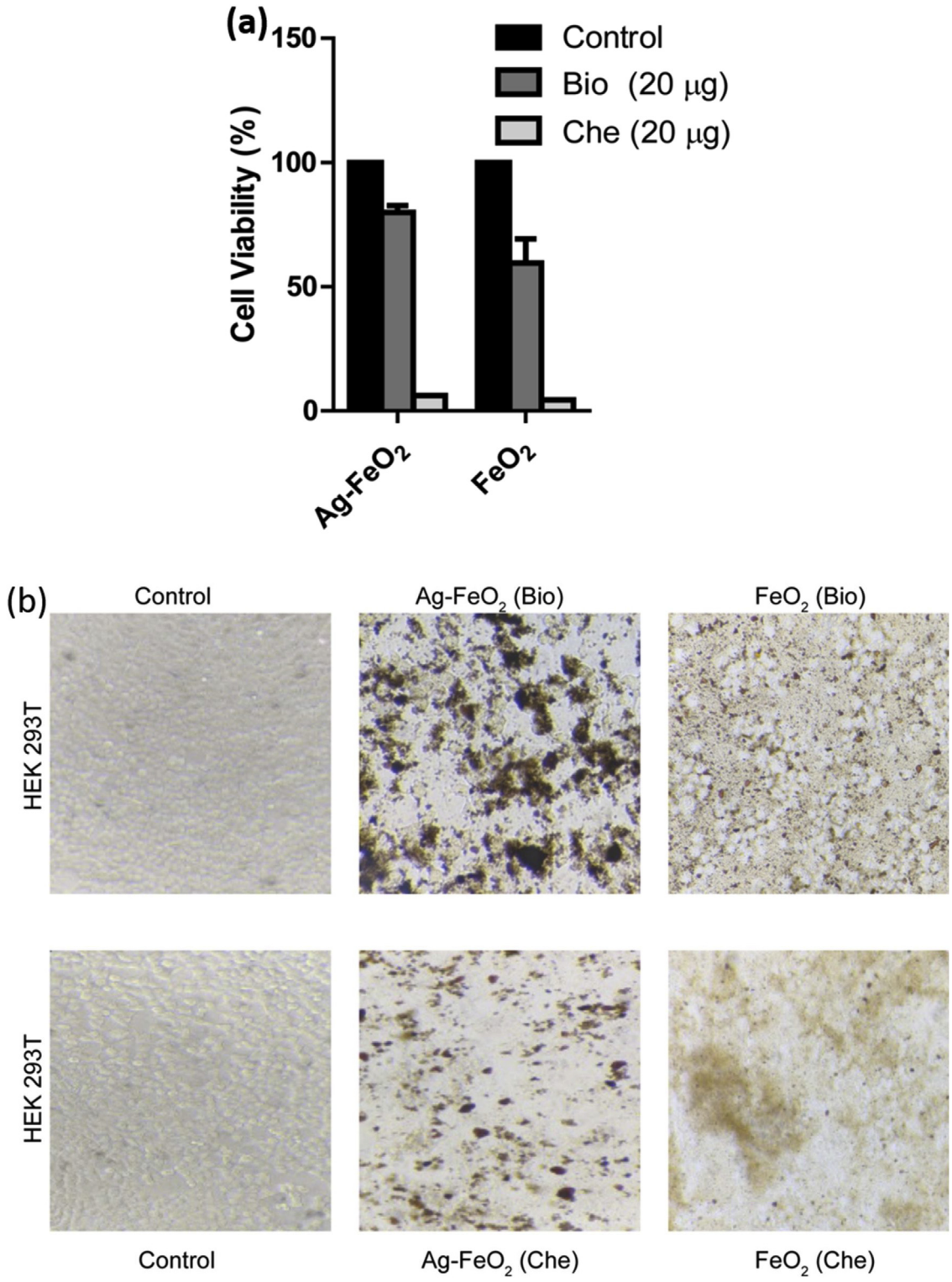

Fig. 8. The *in-vitro* cytotoxicity of different NPs measured by MTT assay. (a) The cytotoxic effect of $AgFeO_2$ (Bio) and FeO_2 NPs synthesised by green co-reduction using *A. blitum* leaves extract and $AgFeO_2$ (Che) and FeO_2 NPs synthesised by chemical co-reduction precipitation method using $NaBH_4$ on non-cancerous human embryonic kidney cell lines (HEK 293 T) after 24 h of treatment were evaluated by mitochondrial activity using the MTT assay. The bar graph represents the mean value of three replicates where cells were treated 20 μg of NPs and cells treated with 10% DMSO were considered as control. (b) HEK 293 T cells treated with different NPs after 24 h incubation. HEK 293 T cells untreated (left panel) and the cells treated with 20 μg of Ag-FeO_2 (middle panel) and with 20 μg of FeO_2 (right panel). Magnification: 20 × . One-way ANOVAs were performed to evaluate significance comparing the both NPs to the control. A value of $p < 0.05$ was considered to be statistically significant as compared to the control. (For interpretation of the references to colour in this figure legend, the reader is referred to the web version of this article).

respectively. Similarly, the growth of *S. aureus* was inhibited by 98% and 79% in the presence of 120 μg [$AgFeO_2$ (Bio)] and [$AgFeO_2$ (Che)] NPs respectively. These results depicted that increase in concentrations of NPs, the final bacterial concentration was decreased [39]. Therefore, the optimum MIC was found to be 100 μg/mL of [AgFeO (Bio)] NPs for *E. coli* and 120 μg/mL of [$AgFeO_2$ (Bio)] NPs for *S. aureus*. Also, significant reduction of CFUs were observed [$AgFeO_2$ (Bio)] NPs against *E. coli* and *S. aureus* (data

not shown). In addition, the results indicate that NPs were more effective against *E. coli* compared to *S. aureus* because of the thin outer membranes of Gram -ve strains as against the Gram + ve strains possessing an additional thick peptidoglycan layer [19]. Therefore, NPs may entered the cell membrane effortlessly compared to other molecules and involves in DNA damage which in turn reduces cell viability [40]. Further, experiments are required to assess the impact and deliverance of metal ions from NPs to a bacterial cell.

3.10. Cytotoxicity studies

The cell viability assay revealed that human embryonic kidney cells treated with NPs synthesised by green co-reduction using *A. blitum* leaves extract showed a slight decrease in the viability than the untreated cells whereas the cells treated with NPs synthesized by chemical co-reduction precipitation method using $NaBH_4$ showed a very poor viability of around 5%. Ag functionalized FeO_2 NPs (Bio) showed a higher viability (~80 %) than the non-functionalized FeO_2 NPs (~60 %) (Bio) when compared to their respective controls (Fig. 8A). The kidney cells were able to survive in the presence of NPs synthesised by green co-reduction and not with NPs synthesized by chemical co-reduction (Fig. 8B). HEK cells were viable till 20 μg of Ag-FeO_2 and FeO_2 and beyond this the cell viability was drastically reduced which depicts that the usage of NPs beyond 20 μg in drug conjugation or biomedical applications might be toxic to the non-cancerous cells.

The particles used in conjugation with drugs and therapies will be rapidly cleared through kidneys [41,42] and hence a study of toxic effects of the NPs having potential biological application on the kidney cell lines provides an insight in to the application as well as the mode of synthesis of NPs. *in vitro* toxicity of several Fe based NPs varies depending on the type of cell lines and the physical properties such as size shape and surface coating of the NPs. Various studies with Iron oxide based NPs at a concentration of 100 μg/ml showed toxicity due to oxidative stress developed by the generation of reactive oxygen species [43]which is evident from our studies also, however Ag functionalised iron NPs synthesized by green reduction in this study showed toxicity at a concentration greater than 200 μg/ml which makes this a promising material for several biomedical applications.

4. Conclusions

Our results clearly showed that [$AgFeO_2$ (Bio)] NPs possess much superior properties compared to [$AgFeO_2$ (Che)]. The characterization results showed that [$AgFeO_2$ (Bio)] NPs have smaller particles size, better surface area and monodispersed as compared to [$AgFeO_2$ (Che)] NPs. The synthesized $AgFeO_2$ (Bio) NPs showed better antimicrobial activities for *E. coli* and *S. aureus* than $AgFeO_2$ (Che) NPs. MIC values for [$AgFeO_2$ (Bio)] was estimated to be 100 μg for *E. coli* and 120 μg for *S. aureus*. The toxicological impacts of [$AgFeO_2$ (Bio)] were tested and compared to [$AgFeO_2$ (Che)] NPs against HEK cells. The results depicted that [$AgFeO_2$ (Bio)] NPs cytotoxicity was lesser than [$AgFeO_2$ (Che)] NPs. The result also depicted that *A. blitum* leaf extract was a better substitute to toxic reducing agents such as $NaBH_4$.AThe results evidently shows that [$AgFeO_2$ (Bio)] NPs exposed better morphology, size, reduced aggregation and high biocidal activity compared to [$AgFeO_2$ (Che)] NPs. Combining the high antibacterial, less toxicity and magnetic properties. Thus [$AgFeO_2$ (Bio)] NPs will be useful for harmless clinical and environmental applications.

AUTHORSHIP STATEMENT

All persons who meet authorship criteria are listed as authors, and all authors certify that they have participated sufficiently in the work to take public responsibility for the content, including participation in the concept, design, analysis, writing, or revision of the manuscript. Furthermore, each author certifies that this material or similar material has not been and will not be submitted to or published in any other publication.

Authorship contributions

Please indicate the specific contributions made by each author (list the authors' initials followed by their surnames, e.g., Y.L. Cheung). The name of each author must appear at least once in each of the three categories below.

Category 1

S.N. Gummadi: Conceptualization,Supervision,Validation,Writing - review & editing. M. Harshiny: Data curation,Methodology, Project, Writing - original draft. P. Santosh Kumar: Methodology, Writing - review & editing. S. Manoj Kumar: Writing - review & editing.

Category 2

Drafting the manuscript: M. Harshiny, P. Santosh Kumar, S. Manoj Kumar, S.N. Gummadi revising the manuscript critically for important intellectual content: M. Harshiny, S.N. Gummadi.

Category 3

Approval of the version of the manuscript to be published (the names of all authors must be listed):

M. Harshiny, P. Santosh Kumar, S. Manoj Kumar, S.N. Gummadi.

Funding

The research was carried out with the funding sponsored by SERB-DST under National Post-Doctoral Fellowshipvide SO. No: PDF/2018/000795.

Declaration of Competing Interest

The authors declare that they have no known competing financial interests or personal relationships that could have appeared to influence the work reported in this paper.

Acknowledgements

The authors would like to acknowledge IIT Madras for the research facilities. SKP and MKS would like to thank MHRD and IIT Madras for the fellowship. MH acknowledges SERB-DST for the National Post-Doctoral Fellowship (SO. No:PDF/2018/000795). Authors would like to acknowledge SAIF-IIT Madras for characterization studies.

Appendix A. Supplementary data

Supplementary material related to this article can be found, in the online version, at doi:https://doi.org/10.1016/j.btre.2020.e00469.

References

[1] P. Koedrith, T. Thasiphu, J. Il Weon, R. Boonprasert, K. Tuitemwong, P. Tuitemwong, Recent trends in rapid environmental monitoring of pathogens and toxicants: potential of nanoparticle-based biosensor and applications, Transfus. Apher. Sci. 2015 (2015) 1–12, doi:http://dx.doi.org/10.1155/2015/510982 Article ID 510982.

[2] L.C. Vitorino, L.A. Bessa, Technological microbiology: development and applications, Front. Microbiol. 8 (2017) 1–23, doi:http://dx.doi.org/10.3389/fmicb.2017.00827.

[3] L. Wang, C. Hu, L. Shao, The antimicrobial activity of nanoparticles: present situation and prospects for the future, Int. J. Nanomed. 12 (2017) 1227–1249, doi:http://dx.doi.org/10.2147/IJN.S121956.

[4] S.S. Patil, U.U. Shedbalkar, A. Truskewycz, B.A. Chopade, A.S. Ball, Nanoparticles for environmental clean-up: a review of potential risks and emerging solutions, Environ. Technol. Innov. 5 (2016) 10–21, doi:http://dx.doi.org/10.1016/j.eti.2015.11.001.

[5] S.K. Murthy, Nanoparticles in modern medicine: state of the art and future challenges, Int. J. Nanomed. 2 (2007) 129–141.

[6] I. Khan, K. Saeed, I. Khan, Nanoparticles: properties, applications and toxicities, Arab. J. Chem. 12 (2019) 908–931, doi:http://dx.doi.org/10.1016/j.arabjc.2017.05.011.

[7] S. Jogaiah, M. Kurjogi, M. Abdelrahman, N. Hanumanthappa, L.S.P. Tran, *Ganoderma applanatum*-mediated green synthesis of silver nanoparticles: structural characterization, and in vitro and in vivo biomedical and agrochemical properties, Arab. J. Chem. 12 (2019) 1108–1120, doi:http://dx.doi.org/10.1016/j.arabjc.2017.12.002.

[8] R. Shanmuganathan, I. Karuppusamy, M. Saravanan, H. Muthukumar, K. Ponnuchamy, V.S. Ramkumar, A. Pugazhendhi, Synthesis of silver nanoparticles and their biomedical applications - a comprehensive review, Curr. Pharm. Des. 25 (2019) 2650–2660, doi:http://dx.doi.org/10.2174/1381612825666190708185506.

[9] H.N. Abdelhamid, A. Talib, H.F. Wu, Facile synthesis of water soluble silver ferrite ($AgFeO_2$) nanoparticles and their biological application as antibacterial agents, RSC Adv. 5 (2015) 34594–34602, doi:http://dx.doi.org/10.1039/c4ra14461a.

[10] N. Sreenivasa, M.P. Bhat, A.C. Udayashankar, T.R. Lakshmeesha, N. Geetha, S. Jogaiah, Biosynthesis and characterization of *Dillenia indica*-mediated silver nanoparticles and their biological activity, Appl. Organomet. Chem. 34 (2020), doi:http://dx.doi.org/10.1002/aoc.5567.

[11] M.C. Stensberg, Q. Wei, E.S. Mclamore, D. Marshall, A. Wei, D.M. Porterfield, M. S. Sepulveda, Toxicological studies on silver nanoparticles: challenges and opportunities in assessment, monitoring and imaging, Nanomed. (Lond.) 6 (2011) 879–898, doi:http://dx.doi.org/10.2217/nnm.11.78.Toxicological.

[12] C.-J.Z. Lingyan Wang, Jin Luo, Shiyao Shan, Elizabeth Crew, Jun Yin, S.W. Brandi Wallek, Bacterial inactivation using silver-coated magnetic nanoparticles as functional antimicrobial agents, Anal. Chem. 83 (2011) 8688–8695, doi:http://dx.doi.org/10.1038/jid.2014.371.

[13] O. Ivashchenko, B. Peplińska, J. Gapiński, D. Flak, M. Jarek, K. Zał ski, G. Nowaczyk, Z. Pietralik, S. Jurga, Silver and ultrasmall iron oxides nanoparticles in hydrocolloids: Effect of magnetic field and temperature on self-organization, Sci. Rep. 8 (2018) 1–14, doi:http://dx.doi.org/10.1038/s41598-018-22426-2.

[14] L.T. Huy, L.T. Tam, T. Van Son, N.D. Cuong, M.H. Nam, L.K. Vinh, T.Q. Huy, D.T. Ngo, V.N. Phan, A.T. Le, Photochemical decoration of silver nanocrystals on magnetic $MnFe_2O4$ nanoparticles and their applications in antibacterial agents and SERS-based detection, J. Electron. Mater. 46 (2017) 3412–3421, doi:http://dx.doi.org/10.1007/s11664-016-5267-x.

[15] Y. Zhao, H. An, J. Feng, Y. Ren, J. Ma, Impact of crystal types of $AgFeO_2$ nanoparticles on the peroxymonosulfate activation in the water, Environ. Sci. Technol. 53 (2019) 4500–4510, doi:http://dx.doi.org/10.1021/acs.est.9b00658.

[16] A.A.H. El-Bassuony, H.K. Abdelsalam, Synthesis, characterization and antimicrobial activity of AgFeO2 delafossite, J. Mater. Sci.: Mater. Electron. 29 (2018) 11699–11711, doi:http://dx.doi.org/10.1007/s10854-018-9268-9.

[17] K. Siedliska, J. Przewoźnik, M. Arczewska, M. Kosmulski, E. Jartych, Effect of annealing temperature on structural properties of the co-precipitated delafossite $AgFeO_2$, Mater. Res. Express 6 (2019), doi:http://dx.doi.org/10.1088/2053-1591/ab26f9.

[18] Y.L.N. Murthy, T. Kondala Rao, I.V. Kasi viswanath, R. Singh, Synthesis and characterization of nano silver ferrite composite, J. Magn. Magn. Mater. 322 (2010) 2071–2074, doi:http://dx.doi.org/10.1016/j.jmmm.2010.01.036.

[19] H. Muthukumar, N.I. Chandrasekaran, S. Naina Mohammed, S. Pichiah, M. Manickam, Iron oxide nano-material: physicochemical traits and in vitro antibacterial propensity against multidrug resistant bacteria, J. Ind. Eng. Chem. 45 (2017) 121–130, doi:http://dx.doi.org/10.1016/j.jiec.2016.09.014.

[20] H. Muthukumar, M. Matheswaran, *Amaranthus spinosus* leaf extract mediated feo nanoparticles: physicochemical traits, photocatalytic and antioxidant activity, ACS Sustain. Chem. Eng. 3 (2015) 3149–3156, doi:http://dx.doi.org/10.1021/acssuschemeng.5b00722.

[21] H. Ahmad, K. Venugopal, K. Rajagopal, S. De Britto, B. Nandini, H.G. Pushpalatha, N. Konappa, A.C. Udayashankar, N. Geetha, S. Jogaiah, Green synthesis and characterization of zinc oxide nanoparticles using *Eucalyptus globules* and their fungicidal ability against pathogenic fungi of apple orchards, Biomolecules 10 (2020) 1–13, doi:http://dx.doi.org/10.3390/biom10030425.

[22] C.L. Keat, A. Aziz, A.M. Eid, N.A. Elmarzugi, Biosynthesis of nanoparticles and silver nanoparticles, Bioresour. Bioprocess. 2 (2015), doi:http://dx.doi.org/10.1186/s40643-015-0076-2.

[23] P. Gupta, D. Chauhan, Green synthesis of silver nanoparticles involving extract of plants of different taxonomic groups, J. Nanomed. Res. 5 (2017).

[24] M. Harshiny, S. AiswaryaDevi, M. Matheswaran, Spiny amaranth leaf extract mediated iron oxide nanoparticles: biocidal photocatalytic propensity, stability, dissolubility and reusability, Biocatal. Agric. Biotechnol. 21 (2019) 101296, doi:http://dx.doi.org/10.1016/j.bcab.2019.101296.

[25] D. Sharma, S. Kanchi, K. Bisetty, Biogenic synthesis of nanoparticles: a review, Arab. J. Chem. 12 (2015) 3576–3600, doi:http://dx.doi.org/10.1016/j.arabjc.2015.11.002.

[26] M. Harshiny, C.N. Iswarya, M. Matheswaran, Biogenic synthesis of iron nanoparticles using *Amaranthus dubius* leaf extract as a reducing agent, Powder Technol. 286 (2015) 744–749, doi:http://dx.doi.org/10.1016/j.powtec.2015.09.021.

[27] J. Jeevanandam, Y.S. Chan, M.K. Danquah, Biosynthesis and characterization of MgO nanoparticles from plant extracts via induced molecular nucleation, New J. Chem. 41 (2017) 2800–2814, doi:http://dx.doi.org/10.1039/c6nj03176e.

[28] U. Sarker, S. Oba, Nutrients, minerals, pigments, phytochemicals, and radical scavenging activity in Amaranthus blitum leafy vegetables, Sci. Rep. 10 (2020) 1–9, doi:http://dx.doi.org/10.1038/s41598-020-59848-w.

[29] A. Al-Asfar, Z. Zaheer, E.S. Aazam, Eco-friendly green synthesis of Ag@Fe bimetallic nanoparticles: Antioxidant, antimicrobial and photocatalytic degradation of bromothymol blue, J. Photochem. Photobiol. B 185 (2018) 143–152, doi:http://dx.doi.org/10.1016/j.jphotobiol.2018.05.028.

[30] K.J. Carroll, D.M. Hudgins, S. Spurgeon, K.M. Kemner, B. Mishra, M.I. Boyanov, L. W. Brown, M.L. Taheri, E.E. Carpenter, One-pot aqueous synthesis of Fe and Ag core/shell nanoparticles, Chem. Mater. 22 (2010) 6291–6296, doi:http://dx.doi.org/10.1021/cm101996u.

[31] P. Berastegui, C.W. Tai, M. Valvo, Electrochemical reactions of $AgFeO_2$ as negative electrode in Li- and Na-ion batteries, J. Power Sources 401 (2018) 386–396, doi:http://dx.doi.org/10.1016/j.jpowsour.2018.09.002.

[32] S.M. Hosseini, H. Hosseini-Monfared, V. Abbasi, Silver ferrite–graphene nanocomposite and its good photocatalytic performance in air and visible light for organic dye removal, Appl. Organomet. Chem. 31 (2017) 1–8, doi:http://dx.doi.org/10.1002/aoc.3589.

[33] D. Tang, G. Zhang, Fabrication of $AgFeO_2$/g-C_3N_4 nanocatalyst with enhanced and stable photocatalytic performance, Appl. Surf. Sci. 391 (2017) 415–422, doi:http://dx.doi.org/10.1016/j.apsusc.2016.06.023.

[34] J.L. Durham, K. Kirshenbaum, E.S. Takeuchi, A.C. Marschilok, K.J. Takeuchi, Synthetic control of composition and crystallite size of silver ferrite composites: profound electrochemistry impacts, Chem Comm. 51 (2015) 5120–5123, doi:http://dx.doi.org/10.1039/c4cc10277k.

[35] E. Casbeer, V.K. Sharma, X.Z. Li, Synthesis and photocatalytic activity of ferrites under visible light: a review, Sep. Purif. Technol. 87 (2012) 1–14, doi:http://dx.doi.org/10.1016/j.seppur.2011.11.034.

[36] X.F. Chuah, K.T. Lee, Y.C. Cheng, P.F. Lee, S.Y. Lu, Ag/AgFeO 2 : An Outstanding Magnetically Responsive Photocatalyst for HeLa Cell Eradication, ACS Omega 2 (2017) 4261–4268, doi:http://dx.doi.org/10.1021/acsomega.7b00698.

[37] N. Cyril, J.B. George, L. Joseph, A.C. Raghavamenon, V.P. Sylas, Assessment of antioxidant, antibacterial and anti-proliferative (lung cancer cell line A549) activities of green synthesized silver nanoparticles from *Derris trifoliata*, Toxicol. Res. 8 (2019) 297–308, doi:http://dx.doi.org/10.1039/C8TX00323H.

[38] A. Alshehri, M.A. Malik, Z. Khan, S.A. Al-Thabaiti, N. Hasan, Biofabrication of Fe nanoparticles in aqueous extract of *Hibiscus sabdariffa* with enhanced photocatalytic activities, RSC Adv. 7 (2017) 25149–25159, doi:http://dx.doi.org/10.1039/c7ra01251a.

[39] K.L. Erik, N. Taylor, K.M. Kummer, N.G. Durmus, T.J.W. Keiko, M. Tarquinio, Superparamagnetic iron oxide nanoparticles (SPION) for the treatment of antibiotic-resistant biofilms, Small. 8 (2012) 3016–3027.

[40] M. Arakha, S. Pal, D. Samantarrai, T.K. Panigrahi, B.C. Mallick, K. Pramanik, B. Mallick, S. Jha, Antimicrobial activity of iron oxide nanoparticle upon modulation of nanoparticle-bacteria interface, Sci. Rep. 5 (2015) 1–12, doi:http://dx.doi.org/10.1038/srep14813.

[41] S.E. McNeil, Nanotechnology for the biologist, J. Leukoc. Biol. 78 (2005) 585–594, doi:http://dx.doi.org/10.1189/jlb.0205074.

[42] Q. Feng, Y. Liu, J. Huang, K. Chen, J. Huang, K. Xiao, Uptake, distribution, clearance, and toxicity of iron oxide nanoparticles with different sizes and coatings, Sci. Rep. 8 (2018) 1–13, doi:http://dx.doi.org/10.1038/s41598-018-19628-z.

[43] S.S. Asad, K.M. Salih, N.Y. Y, Cytotoxic effect of iron nanoparticles in vitro on some cell lines, IJCMG 10 (2017) 71–77.